This document is the accepted manuscript version of the following article:
Joseph, J., Gao, D., Backes, B., Bloch, C., Brunner, I., Gleixner, G., … Gessler, A. (2020). Rhizosphere activity in an old-growth forest reacts rapidly to changes in soil moisture and shapes whole-tree carbon allocation. Proceedings of the National Academy of Sciences of the United States of America PNAS, 117(40), 24885-24892. https://doi.org/10.1073/pnas.2014084117

Biological Sciences

Rhizosphere activity in an old-growth forest reacts rapidly to changes in soil moisture and shapes whole-tree carbon allocation

Jobin Joseph[1#], Decai Gao[1,2 #], Bernhard Backes[3], Corinne Bloch[4], Ivano Brunner[1], Gerd Gleixner[5], Matthias Haeni[1], Henrik Hartmann[5], Günter Hoch[4], Christian Hug[1], Ansgar Kahmen[4], Marco M. Lehmann[1], Mai-He Li[1,2], Jörg Luster[1], Martina Peter[1], Christian Poll[6], Andreas Rigling[1,7], Kaisa A Rissanen[8], Nadine Ruehr[9], Matthias Saurer[1], Marcus Schaub[1], Leonie Schönbeck[1], Benjamin Stern[1], Frank M Thomas[3], Roland A Werner[10], Willy Werner[3], Thomas Wohlgemuth[1], Frank Hagedorn[1*#], Arthur Gessler[1,7*#]

[1] Swiss Federal Research Institute WSL, 8903 Birmensdorf, Switzerland
[2] School of Geographical Sciences, Northeast Normal University, Changchun 130024, China
[3] Geobotany, University of Trier, 54296 Trier, Germany
[4] Physiological Plant Ecology, University of Basel, 4056 Basel, Switzerland
[5] Biogeochemical Processes, Max Planck Institute for Biogeochemistry, 07745 Jena, Germany
[6] Soil Biology, University of Hohenheim, 70599 Stuttgart, Germany
[7] Terrestrial Ecosystems, ETH Zurich, 8092 Zurich, Switzerland
[8] Forest Sciences, University of Helsinki, 00100 Helsinki, Finland
[9] Plant Ecophysiology, Karlsruhe Institute of Technology, 82467 Garmisch-Partenkirchen, Germany
[10] Agricultural Sciences, ETH Zurich, 8092 Zurich, Switzerland

* corresponding authors: Arthur Gessler: arthur.gessler@wsl.ch; phone: 00 41 44 739 28 18; Frank Hagedorn: frank.hagedorn@wsl.ch; phone: +41 44 739 24 63; Swiss Federal Research Institute WSL, 8903 Birmensdorf, Switzerland
# these authors contributed equally to this paper

Keywords

Drought, Drought release, ^{13}C pulse labelling, sink control

Significance

Climate change increases the frequency of drought events and leads to higher variability in precipitation. Drought impairs rhizosphere (root and the root-associated

microbiome) functioning in trees and leads to a reduced assimilate supply belowground. It remains unclear if rhizosphere and thus whole tree functioning can quickly recover after drought release. We show that rhizosphere metabolic activity in previously drought-exposed 100-year-old Scots pine increased in response to subtle soil moisture increases (induced by light rainfall). As a consequence of this activity change, the belowground allocation of new assimilates was immediately stimulated. Even light rainfall events can lead to a fast recovery of rhizosphere functioning and the increased C and energy demand is instantly met by altered whole tree assimilate allocation.

Abstract

Drought alters carbon (C) allocation within trees, thereby impairing tree growth. Recovery of root and leaf functioning and prioritized C supply to sink tissues after drought may compensate for drought-induced reduction of assimilation and growth. It remains unclear if C allocation to sink tissues during and following drought is controlled by altered sink metabolic activities or by the availability of new assimilates. Understanding such mechanisms is required to predict forests' resilience to a changing climate.

We investigated the impact of drought and drought release on C allocation in a 100-year-old Scots pine forest. We applied $^{13}CO_2$ pulse labelling to naturally dry control and long-term irrigated trees and tracked the fate of the label in above- and belowground C pools and fluxes.

Allocation of new assimilates belowground was ca. 53% lower under non-irrigated conditions. A short rainfall event, which led to a temporary increase in the soil

water content (SWC) in the topsoil, strongly increased the amounts of C transported belowground in the non-irrigated plots to values comparable to those in the irrigated plots. This switch in allocation patterns was congruent with a tipping point at around 15% SWC in the response of the respiratory activity of soil microbes.

These results indicate that the metabolic sink activity in the rhizosphere and its modulation by soil moisture can drive C allocation within adult trees and ecosystems. Even a subtle increase in soil moisture can lead to a rapid recovery of belowground functions that in turn affects the direction of C transport in trees.

Introduction

While climate projections predict a higher frequency of extreme weather events, such as hot drought periods (1) but also intermittent heavy rainfall (2), we have limited knowledge on how tree C allocation (the distribution of assimilates among tree organs), which is important for whole tree functioning, is impaired by water restriction (3, 4). Moreover, we lack information on the extent to which C allocation can recover after drought (5, 6). There are several reasons for this knowledge gap: (i) Most experiments on C allocation dynamics have investigated the impact of extreme drought events on trees and ecosystems (7-9) but neglected the more common subtle variations in soil moisture occurring in natural ecosystems. For example, a simulation of the European 2003 drought – assumed to represent an extreme event – in a range of forest ecosystems showed that the soil water reduction was moderate (10) compared to the drought conditions created in most experimental studies on C allocation (e.g., 3, 11). (ii) There are indeed many studies that address small but realistic variations in soil moisture but most of these have solely focused on

aboveground responses of tree C relations (12, 13) or integrated whole ecosystem CO_2 exchange impacts (14, 15) while not taking into account interactions and linkages between shoots and roots and the associated rhizosphere microbiome. For juvenile trees, though, C transfer between shoots, roots and rhizosphere microbes was found to be crucial for both plant and microbial functioning under stress (9).

Concerning the aboveground-belowground linkage, drought moderately increased C allocation to roots in some studies (16) while reduced allocation was reported in others (17). These inconsistencies are difficult to interpret because the mechanisms that control C allocation within plants and ecosystems are largely unknown; this is a critical knowledge gap considering that ca. 50% of the energy demanding processes in the rhizosphere – including roots, mycorrhizal fungi and bacteria – are fuelled by recently assimilated C (18). The mechanisms of C allocation under water stress remain particularly unexplained in mature trees and hence in old-grown forests due to a lack of experimental studies, although their understanding is crucial for predicting forest functioning in a drier climate.

The common understanding of the impact of water stress on tree C allocation is that reduced photosynthesis during drought determines the availability of carbohydrates (source control) and can lead, together with impaired phloem transport (19), to reduced C allocation to sink tissues. More recent research indicates control of plant C allocation but also of C assimilation by sink metabolic activity (sink control). In this respect, the belowground sink activity of roots (11) and associated microorganism (20) seems to play a decisive role. Mild water deficit can increase root growth and metabolic activity to improve water foraging and consequently increases belowground C demand, leading to higher assimilate transport belowground (21). In contrast, drought that exceeds a critical level inhibits belowground metabolism and thus

reduces belowground C demand leading to less C being directed to the rhizosphere (22). Reduced C sink strength can even lead to a down-regulation of photosynthesis (20). In tree saplings, this was assumed to be a result of the acclimation of C assimilation to the reduced sink demand and occurred with a delay of two weeks after the reduction of the belowground sink activity (11) probably as result of leaf sucrose accumulation (cf. 23).

Sink control has also been observed directly after drought release: in beech saplings, increased root activity and thus C demand resulted in the prioritized transport of new assimilates belowground, and only in a second step, with a delay of weeks, did photosynthesis re-adjust to the new conditions and to the higher C demand (11). If the tree C balance after drought release had been under source control, first photosynthesis and only later belowground C transport and sink activity would have increased. So far, experimental studies typically only include young trees and it is unknown if these mechanisms also operate in mature trees in old-growth forests which store large amounts of reserves that may buffer C allocation.

Rhizosphere microorganisms are an important part of the belowground C sink in ecosystems (24), and the C transfer between forest plants and soil microorganisms is known to be negatively affected by hot droughts (9). It is not fully understood, however, whether drought itself suppresses microbial activity or rather a lower C transfer from plants to the rhizosphere microbiome is the driving force. Moreover, it is not clear if and to what extent rhizosphere microorganisms and their activity are involved in the sink control of whole-tree C allocation.

Taking advantage of a long-term (15 years) precipitation manipulation (irrigation) experiment in a dry inner Alpine valley in Switzerland (25) and the natural fluctuations of drought and rainfall, we studied the effects of drought and intermittent drought

release by a precipitation event on C allocation in a 100-year-old Scots pine forest. We applied $^{13}CO_2$ pulse labelling to 10 mature trees and traced the flux of newly assimilated C from needles into branch, trunk, root and soil microbial biomass pools and into above- and belowground respiration **(Fig. 1)**. We hypothesized that the soil moisture deficit in the dry non-irrigated plots during periods without rainfall would result in less allocation of recent assimilates belowground and a higher proportion remaining in aboveground tree tissues and fluxes compared to irrigated trees **(SI Appendix, Fig. S1)**. We further predicted that short rainfall events, that increase soil moisture above a critical threshold value – allowing increased rhizosphere metabolic activity – would temporarily lead to prioritized transport of assimilates belowground in the normally xeric plots. We expected that rhizosphere sink activity, including the metabolism of roots and associated microorganisms, would control the whole-tree C allocation patterns. As sink control influences photosynthesis with a delay of weeks after changes in sink activity and C allocation patterns (11), we hypothesized that short rainfall events would have only minor effects on C assimilation **(SI Appendix, Fig. S1)**.

Results and Discussion

We started a first ^{13}C labelling campaign at the end of August 2017 after >2 weeks of almost no rainfall (<0.9 mm) **(SI Appendix, Fig. S2a)**, when soil water content in the non-irrigated plots approached values < 15% below 2 cm soil depth **(SI Appendix, Figs. S2, S3)**. Even though leaf water potential was significantly lower (p = 0.007) in the dry non-irrigated compared with the irrigated plots **(Tab. 1, SI Appendix, Fig. S4)**, no significant differences were observed for stomatal conductance, transpiration, photosynthetic rate **(Tab. 1, SI Appendix, Fig. S5)** or total

^{13}C assimilation during pulse labelling **(Tab. 1, SI Appendix, Tab. S1)**. It took approximately six days for the ^{13}C assimilated in the canopy of the 10- to 15-m-tall trees to be transferred to the rhizosphere (**Fig. 2 b-e**). Dry conditions in the non-irrigation treatment significantly reduced the allocation of ^{13}C to belowground C sinks, including non-structural (sugar and starch) and structural C pools in roots, the soil microbial biomass (irrigation effect on ^{13}C allocation to belowground pools: p = 0.01, **Tab. 1**) and cumulative soil respiratory flux (irrigation effect: p = 0.009, **Tab. 1**): 30 days after labelling the ^{13}C transferred to these belowground sinks was by 53% lower in non-irrigated compared with irrigated trees (**Fig. 3, SI Appendix, Tab. S2**). In contrast to the generally lower transport of new assimilates belowground, mycorrhizal root tips showed comparable ^{13}C incorporation in non-irrigated and irrigated plots **(SI Appendix, Fig. S6).** In forest understorey ecosystems it was recently observed that smaller amounts of recent assimilates were transported belowground under drought but that rhizosphere microbes, including mycorrhizal fungi, obtained a relative larger proportion of these assimilates thus partially compensating for the change in plant allocation patterns (9). This suggests that plants continue to support the rhizosphere microbiome with recently fixed C during drought to help to sustain its function in water and nutrient acquisition (cf. 26).

Our finding of reduced export to the belowground compartment under drought is in agreement with the longer mean residence time (MRT) of the leaf sugars used as respiratory substrates. The fast turn-over C pool in the canopy of drought-exposed non-irrigated trees had an MRT of 3.8 days, whereas it was only 0.7 days in irrigated trees (**SI Appendix, Tab. S3**). This range is consistent with values from other studies on pine (27, 28), and comparable increases in MRT as a result of drought have been observed in European beech seedlings (3). The authors of the latter study

hypothesized that reduced sink activity, e.g. in the roots was not responsible for the higher MRT, but rather a higher demand for osmotically active substances in the leaves together with impaired phloem loading (29). More recently, however, an assessment of temporal changes in root and shoot metabolite concentrations and metabolic activity in beech seedlings demonstrated that not only drought but also drought release initially impacted sink activity in the roots, and only with a delay did sink activity feed back on the source organ (11). The reduced sink activity during drought led to reduced leaf phloem loading and increased metabolite accumulation in the leaves and the increased root activity after drought to increased belowground transport but not to an immediate stimulation of photosynthesis.

Our second ^{13}C labelling application after the short rainfall event (8 mm; **SI Appendix, Fig. S2a**) highlights that, in a 100-year-old forest, even subtle but significant changes in soil water availability in the uppermost soil layer (precipitation effect: p = 0.04, **Tab. 1**) rapidly increased rhizosphere sink activity and C allocation belowground, demonstrating that sink control mechanisms acting also in old trees. The rainfall event increased SWC in the uppermost 5 cm of the dry non-irrigated plots to values similar to those in irrigated plots prior to the rainfall (**SI Appendix, Fig. S3**), while SWC in deeper layers (10 and 80 cm) was less affected (**SI Appendix, Fig. S2 b, c**). This soil moisture increase led to a significant increase in: (i) the absolute $^{13}CO_2$ soil respirational flux (**Fig. 2 b, c**), and (ii) the incorporation of ^{13}C label into the soil microbial (i.e. bacterial and fungal) biomass (**Fig. 2 d, e**) in the non-irrigated compared with the irrigated plots, resulting in a significant interaction between precipitation and irrigation ($p < 0.05$). The ^{13}C balance calculated for 30 days after labelling showed that relative belowground allocation in trees labelled after the rainfall event was higher in the non-irrigated than in irrigated plots (**Fig. 3, SI Appendix, Tab. S2**). Trees in the

non-irrigated plots significantly increased relative allocation to roots and the rhizosphere, while belowground allocation in the irrigated plots remained unaffected by the rainfall event (indicated by a significant irrigation x precipitation interaction, p = 0.006 for belowground pools and p = 0.04 for soil respiration; **Tab. 1**).

To explore the mechanism behind this rapid change in the partitioning of recent assimilates between above- and belowground compartments, we estimated the moisture dependency of microbial soil respiration (and thus microbial activity) from root-free soil adjusted to different soil moisture levels in the laboratory. Results revealed a clear tipping point of microbial respiration at around 15% SWC (**Fig. 4a**). Such soil moisture dependent tipping points in soil microbial activities have been observed in various other drought studies (30). Total respiratory ^{13}C soil flux in the field reflecting the use of new assimilates by the rhizosphere showed a similar moisture dependency than microbial activity (**Fig. 4b**). This congruence suggests the existence of a soil moisture depending tipping point for the sink activity of the entire root-rhizobiome system increasing the use of new assimilates and thus the allocation to roots and rhizosphere. Even though the number of pulse-labelled trees was rather low and only one rainfall event was examined (three non-irrigated and three irrigated trees before and two of each treatment after the rainfall event), 61% of the moisture dependency of the ^{13}C flux could be explained by the threshold-type Boltzmann function fitted to microbial respiration in soils without roots (**Fig. 4b)**. At the same time, total ^{13}C label uptake by trees and leaf-level photosynthetic rates did not differ significantly between the treatments (**Tab. 1, SI Appendix, Tab. S1)**. Consequently, the root-rhizobiome activity and whole-tree assimilate allocation patterns changed rapidly after a short rainfall event without a change in CO_2 assimilation. These findings

indicate that belowground metabolic activity and its modulation by soil moisture drove C allocation and transport within the adult trees and the whole forest ecosystem.

The re-activation of the rhizosphere sink by intermittent rainfalls likely depends on both, rainfall patterns and vertical distribution of the rhizosphere. Our mature pine forest had 60% of its entire fine root system in the uppermost 10 cm (measured down to 80 cm (31), which corresponds to other temperate forest ecosystems (32). Fine roots from the uppermost soil layer are physiologically more active and more strongly colonized with mycorrhizal fungi as compared to deeper roots that ensure the water supply of trees during severe droughts (33-35). We thus assume that the observed rewetting of the topsoil affected the largest part of the metabolically active rhizosphere, but in soils with deeper fine root systems such as Mediterranean forests (36) responses of the rhizosphere sink to intermittent rainfalls might be less pronounced.

In a previous study at the same site (25), we showed that concentrations of soluble sugars in all tree compartments (needles, stems, and roots) were comparable between non-irrigated and irrigated trees in summer and autumn, when soil moisture was clearly lower in the non-irrigated plots. It was concluded that carbohydrate supply and demand were balanced over the long term. Here, we observed a strong and significant depletion of the soluble sugars in the roots in the non-irrigated plots (relative to values in the irrigated plots) shortly after the rainfall event ($p < 0.05$), and only two weeks later the pool was replenished (**Fig. 2a**). This suggests that despite long-term adjustments of the C balance, short-term fluctuations can occur due to fast increases in belowground metabolic activity (**Fig. 4**), leading to a transient imbalance of supply and demand. Consequently, the increased C demand explains the higher proportion of new assimilates transported belowground and corroborates the idea of sink control of C allocation. Notably, changes in C allocation driven by the root-rhizobiome system

act on very short time scales: even though the rainfall event occurred shortly after the first ^{13}C labelling the belowground allocation of ^{13}C remained low in the non-irrigated plots (**Fig. 3**). Only the new assimilates formed right after the rainfall event were differently distributed, supporting the importance of new assimilates in fueling belowground processes (18) and indicating that the distribution patterns of new assimilates are kept stable after the initial allocation.

Our results provide the first evidence for adult trees that drought reduces the allocation of recent assimilates belowground. Our findings also demonstrate that mature forest ecosystems in xeric environments can exhibit highly dynamic short-term changes in assimilate distribution: sudden increases in soil water availability in the uppermost soil layer can result in a boost of belowground metabolic activity and carbohydrate depletion in roots which, in turn lead to strongly increased assimilate transport to the rhizosphere. We acknowledge that we only captured a single recovery event in a single ecosystem and thus we are cautious in extrapolating our results to other forest ecosystems with different species and to droughts and subsequent recovery events of different magnitudes and duration. As a consequence, more experiments on C allocation in various old-growth forest ecosystems under a range of environmental conditions are needed. Our results, however, provide first indications that fluctuations in soil water availability in dry sites allow belowground processes to recover fast after rainfall events, and the increased C and energy demand is immediately reflected in changes in whole-tree and ecosystem assimilate allocation patterns. The moisture-sensitive sink strength of the rhizosphere, including roots and the root-rhizobiome system represents an important but so far overlooked driver of forests' responses to drought and drought release, altering the direction of carbon transport in trees and ultimately modifying physiological acclimation to drought.

Materials and Methods

Experimental site

The ^{13}C pulse labelling experiment was carried out with approximately 100-year-old Scots pine (*Pinus sylvestris* L.) trees growing in a naturally regenerated forest (Pfynwald) in the dry inner-Alpine valley of the river Rhone, one of the driest parts of the European Alps (46° 180 N, 7° 360 E, 615 m a.s.l.). The soil is a shallow 20 cm thick Pararendzina (37), annual mean temperature is 10.1°C, and annual precipitation is ca. 600 mm. In the recent past, the forest has been subjected to drought- and heat-induced forest mortality (38). Since 2003 (for 15 years), four plots of 25 x 40 m^2 each have been irrigated at night with 600 mm yr^{-1} between April and October (25), thus doubling the amount of precipitation per year and removing soil water limitation. Four corresponding non-irrigated plots serve as naturally dry controls (for more details see **SI Appendix, Supplementary Methods**).

^{13}C pulse labelling

In late summer 2017, 10 (five naturally non-irrigated and five irrigated) 100-year-old Scots pine trees were $^{13}CO_2$ labelled (**Fig. 1**). Three pairs of trees were pulse labelled during a dry period (little precipitation within >2 weeks before pulse labelling) on consecutive days, and another two pairs were labelled immediately after a short rainfall event (see **SI Appendix, Fig. S2**). Transparent plastic chambers enclosing the whole crown were erected from scaffolds and temperature and relative humidity were kept at ambient levels using a mobile air conditioning system (**Fig. 1**). At each labelling event, two trees, one irrigated and one non-irrigated, were labelled simultaneously. After sealing the chamber CO_2 with >99 atom% ^{13}C (Cambridge Isotopes, Tewksbury, MA, USA) was released into the chamber over a period of 3.5h, increasing the $^{13}CO_2$

concentration to 1000–1500 ppm, with a $\delta^{13}C$ of up to 250,000 (‰) (measured with an isotope laser spectrometer (LGR, CCIA 46d, LosGatos Research Ltd, San Jose, CA, USA); **SI Appendix, Figs. S7, S8**). Afterwards the chambers were removed, and large industrial blowers set up on the forest floor were used to rapidly remove non-assimilated $^{13}CO_2$.

Measurements of soil water contents, leaf gas exchange and canopy, stem and soil $^{13}CO_2$ efflux

Soil water: Volumetric soil water content (SWC) at depths of 10 and 80 cm was measured every 15 min across the eight plots of the experimental site using soil moisture sensors (ECH$_2$O EC-5, Decagon Devices, Pullman, WA, USA). In addition, soil water content was repeatedly determined gravimetrically at 0-2 cm, 2-5 cm and 5-10 cm depth by sampling soils at 12 locations around each of the pulse-labelled trees, bulking the samples, and drying them at 105°C.

Gas exchange: Leaf-level gas exchange (transpiration (E), stomatal conductance (g_s), assimilation (A)) was measured with a portable gas exchange measurement device (LI-COR 6400; LI-COR, Lincoln, NE, USA) before and after the rainfall event in the upper third and thus fully sun-exposed part of the canopy. Four trees of each treatment (irrigated and non-irrigated) and needles from three twigs of each tree were measured before and after the rainfall event. The CO_2 concentration inside the cuvette was set to 400 ppm, cuvette temperature to 25°C, photosynthetic photon flux density to 1000 µmol m^{-2} s^{-1}. Relative humidity was adjusted to ambient conditions and flow rate set to 650 µmol s^{-1}. Branch water potential was determined with a Scholander pressure chamber (39) in six trees per treatment (and with three

branches per tree) before the rainfall event. Both, leaf-level gas exchange and branch water potential were determined around midday.

$^{13}CO_2$ fluxes (high resolution measurements): For tracking the temporal patterns of ^{13}C allocation, canopy (leaves and branches), stem and soil $^{13}CO_2$ fluxes of trees labelled before the rainfall event (n = 6) were measured with an hourly resolution for 20 consecutive days after pulse labelling (**SI Appendix, Fig. S9**) by coupling three stable isotope laser spectrometers (LGR, CCIA 46d, LosGatos Research Ltd, San Jose, USA) with custom-made automated soil, leaf and branch chambers designed for gas exchange measurements(40) (**Fig. 1**). Soil chambers were installed at a distance of 0.5 m from the stem of each tree, stem chambers were attached at the stem approx. 1.5 m above ground and branches from the upper third of the canopy were inserted into the canopy chambers. We assumed no strong gradients in light, VPD or other environmental conditions within the sparse canopy of the trees at our stand. In a Scots pine stand with a comparable structure no intra-canopy gradients in gas exchange were observed (41) and thus we are confident that the branches selected were representative for the whole canopy.

Chambers were programmed to be open during non-measurement intervals to avoid CO_2 accumulation and increases in temperature and humidity inside the chamber system. In the measurement mode they were closed, and the respired CO_2 was allowed to accumulate for five minutes when the gas stream was passed to the isotope laser spectrometer. The $\delta^{13}C$ value of respired CO_2 was calculated as a two end-member mixture of ambient and respired CO_2 sampled in the chamber over time (42) and fluxes were determined from the linear CO_2 concentration increase over time and were related to the surface area of the leaves (canopy), stem or soil. For the ^{13}C mass balance calculation (see below) for canopy respiration fluxes, only measured

nighttime CO_2 fluxes and $\delta^{13}C$ values were considered, and daytime fluxes were calculated according to the temperature dependency of nighttime fluxes and the actual temperature. Daytime $\delta^{13}C$ values were extrapolated from the time course of nighttime values with an exponential decay function.

Laser-based measurements were used for estimating (i) the time-integrated canopy and stem fluxes for the mass balance calculation (see below) and (ii) the mean residence time (MRT) of recent assimilates in the canopy, stem and the soil (**SI Appendix, Tab. S3**). Exponential decay models were fitted in the phase of label decrease according to (27) and two labile C pools (i.e. soluble sugars and starch) with different MRT values were assumed.

$^{13}CO_2$ fluxes (low resolution measurements): For quantifying soil ^{13}C fluxes from the entire rhizosphere of each of the 10 pulse-labelled trees (6 trees before the precipitation and 4 trees afterwards), we installed soil collars of 10 cm diameter along three transects at distances of 0.5, 1.0, 1.5, 2.0, 3.0, 4.0, 6.0 and 8.0 m from the tree stems. Soil respiration (R_S) was measured at up to a daily resolution with a soil CO_2 flux system LI-8100A with a LI 8100-102 survey chamber (LI-COR, Lincoln, USA) placed on the soil collars over 30 days following pulse labelling. For measuring $\delta^{13}C$ values of soil-respired CO_2, the collars were closed with lids and gas samples were taken with syringes after 15-20 min. In addition, ambient air close to the soil surface was collected during each sampling period. In gas samples, the $\delta^{13}C$ values and the CO_2 concentration were analysed with a GasBench II (modified according to (43)) coupled to a Delta Plus^{XP} isotope ratio mass spectrometer (IRMS) (ThermoFinnigan, Bremen, Germany). The $\delta^{13}C$ value of the respired CO_2 was calculated as a two end-member mixture of ambient and respired CO_2 sampled in the chamber after 15-20 min (42).

The low-resolution soil fluxes were used to estimate the soil ^{13}C fluxes integrated over time- and space for each of the pulse-labelled tree (see below).

Moisture dependency of microbial soil respiration

The moisture dependency of heterotrophic soil respiration was determined for 20 g of root-free soil samples from 0-2, 2-5 and 5-10 cm depth, which were first dried at room temperature and then rewetted to the desired water content (n=6 per moisture content). Carbon mineralization was measured in gas-tight glass jars of 500 ml volume, equipped with an opening rubber septum through which 8 ml of gas samples were extracted after 24, 48, 72, and 96 h. These samples were injected into pre-evacuated 4 ml exetainers and analysed for CO_2 concentrations by gas chromatography (Agilent 7890, Agilent Technologies Inc., Santa Clara, CA, USA).

Determination of ^{13}C recovery in above- and belowground pools

Sampling and pre-processing: Needle (combined current and previous year's cohorts) and branch samples were collected in the upper third of the canopy 1 h before pulse labelling, directly after labelling (0 h) and until 30 days after labelling (cf. **SI Appendix, Figs. S10, S11**). The needles were removed from the branches, transferred into paper bags, microwaved to denature all enzymes and then oven dried. The branch material was stored in exetainers in liquid nitrogen and was later oven dried. Stem wood samples plus stem phloem were taken 10 and 30 days after pulse labelling (**SI Appendix, Figs. S10, S11**). For stem samples, 10-mm increment cores were taken with an increment borer (Haglöf Sweden AB, Långsele, Sweden) at three locations in a 120° angle around the stem at breast height at each sampling time point. The core samples were transferred into exetainers and immediately stored at -20°C. After drying, the outer 30 tree rings and the phloem were used for further analysis. For

root sampling, coarse roots were traced from their insertion point into the stem, excavated from the soil, microwaved, oven dried and homogenized. Water-soluble compounds and starch were extracted from subsamples of all tree tissues (see **SI Appendix, Supplementary Methods**). To assess mycorrhizal root tips, three soil cores with a diameter of 2 cm were randomly sampled from the upper 0-10 cm of the soil (the main rooting horizon (31)) in the immediate vicinity of each tree 0, 7, and 14 days after labelling, and the samples were pooled per tree. Vital mycorrhizal root tips were immediately collected from the soil cores under a stereomicroscope and kept at −70°C until processing. All bulk tree tissue samples (needles, wood, roots, mycorrhizal root tips), ground to a fine powder after drying at 80°C, using a steel ball mill (MM 400 Retsch GmbH, Haan, Germany) for further analyses. For the assessment of C concentrations and $\delta^{13}C$ in the bulk organic matter of tree tissues, starch and water soluble compounds (WSC), ca. 0.6 mg of the homogenized and dried material was weighted into tin capsules for further isotope analysis (see **SI Appendix, Supplementary Methods**). To quantify soil microbial biomass, 12 soil cores of 2 cm diameter were sampled within 1 m distance of each tree and bulked. All roots were removed from the soil, and the samples were then immediately frozen and later analysed for soil microbial biomass using the chloroform fumigation extraction method. Both the concentration and isotopic signature of extracted organic C from non-fumigated and fumigated samples were determined by oxidizing extractable C to CO_2 (44) and measuring the $^{13}CO_2$ with an isotope ratio mass spectrometer (IRMS) (GasBench II coupled to a Delta V plus; ThermoFinnigan, Bremen, Germany) and calculated as described previously assuming a conversion factor of 0.45 (45).

Soluble sugars in roots

Concentrations of soluble sugars in roots (**Fig. 2a**) were determined according to (46) as described in detail by (25)**.**

445

^{13}C mass balance estimation

The amount of ^{13}C taken up by the trees (calculated based on the amount of 99%^{13}C-CO_2 supplied to the pulse labelling chamber from the gas cylinder; see Tab. 450 S1) and recovered in the different tree pools, the soil microbial biomass, and the CO_2 released from branches, stem, and soil were used for a ^{13}C mass balance estimation of individual trees and their related rhizosphere. To assess the total ^{13}C enrichment in tree pools as a result of labelling, total biomass (g) of the different plant compartments (needles, branches, stem, and roots) was calculated for each tree from allometric 455 functions specific for *P. sylvestris* using tree height and diameter at breast height (DBH) as input parameters (47). In a next step, total C of each biomass pool ($C_{pool;}$ g) was calculated by multiplying the biomass by the specific C content (%) of the pool as determined by the isotope measurements. We performed these calculations separately for bulk C and for non-structural C (NSC = starch plus WSC). From the 460 difference between bulk C and NSC we computed the structural C pool (SC) (**SI Appendix, Tab. S2**). The C pool of the microbial biomass (0-10 cm depths) was estimated by multiplying microbial biomass with the mass of soil on an area base using measured soil bulk densities. ^{13}C excess, i.e. the ^{13}C enrichment due to labelling expressed in atom% (**SI Appendix, Supplementary Methods** and (3)) 30 days after 465 the pulse labelling was multiplied by the C pools of tree and microbial biomass. For the scaling of the ^{13}C excess of the microbial biomass to the circular area around each tree, we linked them to the decline of soil-respired $^{13}CO_2$ with distance from the stems. The CO_2 flux rates from the canopy and stem (hourly resolution) were multiplied by the ^{13}C excess and the surface area and integrated over the 30 days after the pulse

labelling (see **SI Appendix, Supplementary Methods**). Needle area was determined from the needle mass obtained from tree allometric functions (47) and the specific leaf area determined for every tree and we assumed gas exchange in the canopy chamber to be representative of gas exchange of the whole canopy. Stem area was determined from DBH and tree height assuming the stem to be a truncated cone with the upper diameter being 5% of DBH. For estimating soil $^{13}CO_2$ flux from the entire rhizosphere of each tree, we interpolated linearly between the fluxes from adjacent soil collars placed at various distances from the tree stems (see **Fig. 1**) measured at daily resolution and integrated them over time. ^{13}C in pools and fluxes were related to the ^{13}C applied during pulse labelling to obtain recovery rates (see **SI Appendix, Supplementary Methods**), and the relative allocation to different pools and fluxes was calculated (**Fig. 3, SI Appendix, Supplementary Methods, Tab. S2**).

Statistical analysis

Data were analysed by fitting linear mixed effects models with maximum likelihood using the lme function in the nlme package (R version 3.1.2.). For the entire study period, treatment (irrigated vs. non-irrigated) and date of measurement (before and after the precipitation event) were used as fixed effects in the models and individual tree was included as a random effect. The corAR1 function in the nlme package was included in the models to account for repeated measurements with a first-order autoregressive covariate structure. In all final models, the dependent variables were log or square-root transformed to achieve normality and homoscedasticity of the residuals.

Acknowledgements

This work was funded by the Swiss National Science Foundation (SNF) under contract numbers 31003A_159866 and 310030_189109 (to A.G.) and by the Sino Swiss Science and Technology Cooperation (EG 09-122016) (to D. G. and F. H.)

References

1. Allen CD, Breshears DD, & McDowell NG (2015) On underestimation of global vulnerability to tree mortality and forest die-off from hotter drought in the Anthropocene. *Ecosphere* 6(8):129.
2. IPCC (2013) *Climate Change 2013: The Physical Science Basis. Contribution of Working Group I to the Fifth Assessment Report of the Intergovernmental Panel on Climate Change* (Cambridge University Press, Cambridge, United Kingdom and New York, NY, USA) p 1535.
3. Ruehr NK*, et al.* (2009) Drought effects on allocation of recent carbon: from beech leaves to soil CO2 efflux. *New Phytol* 184(4):950-961.
4. Hartmann H, McDowell NG, & Trumbore S (2015) Allocation to carbon storage pools in Norway spruce saplings under drought and low CO2. *Tree Physiology* 35:243-252.
5. Galiano L*, et al.* (2017) The fate of recently fixed carbon after drought release: towards unravelling C storage regulation in Tilia platyphyllos and Pinus sylvestris. *Plant, Cell & Environment* 40(9):1711-1724.
6. Trugman AT*, et al.* (2018) Tree carbon allocation explains forest drought-kill and recovery patterns. *Ecology Letters* 21(10):1552-1560.
7. Doughty CE*, et al.* (2015) Drought impact on forest carbon dynamics and fluxes in Amazonia. *Nature* 519(7541):78-82.
8. Aaltonen H, Lindén A, Heinonsalo J, Biasi C, & Pumpanen J (2016) Effects of prolonged drought stress on Scots pine seedling carbon allocation. *Tree Physiology* 37(4):418-427.
9. von Rein I*, et al.* (2016) Forest understory plant and soil microbial response to an experimentally induced drought and heat-pulse event: the importance of maintaining the continuum. *Global Change Biology* 22(8):2861-2874.
10. Felsmann K*, et al.* (2017) Responses of the structure and function of the understory plant communities to precipitation reduction across forest ecosystems in Germany. *Annals of Forest Science* 75(1):3.
11. Hagedorn F*, et al.* (2016) Recovery of trees from drought depends on belowground sink control. *Nature Plants* 2:16111.
12. Zweifel R, Zimmermann L, Zeugin F, & Newbery DM (2006) Intra-annual radial growth and water relations of trees: implications towards a growth mechanism. *Journal Of Experimental Botany* 57(6):1445-1459.
13. Xia JB, Zhao ZG, Sun JK, Liu JT, & Zhao YY (2017) Response of stem sap flow and leaf photosynthesis in Tamarix chinensis to soil moisture in the Yellow River Delta, China. *Photosynthetica* 55(2):368-377.
14. Greco S & Baldocchi DD (1996) Seasonal variations of CO2 and water vapour exchange rates over a temperate deciduous forest. *Global Change Biology* 2(3):183-197.

15. Pilegaard K, Hummelshøj P, Jensen NO, & Chen Z (2001) Two years of continuous CO2 eddy-flux measurements over a Danish beech forest. *Agricultural and Forest Meteorology* 107(1):29-41.
16. Poorter H*, et al.* (2012) Biomass allocation to leaves, stems and roots: meta-analyses of interspecific variation and environmental control. *New Phytologist* 193(1):30-50.
17. Meier I & Leuschner C (2008) Genotypic variation and phenotypic plasticity in the drought response of fine roots of European beech. *Tree Physiology* 28(2):297-309.
18. Högberg P*, et al.* (2001) Large-scale forest girdling shows that current photosynthesis drives soil respiration. *Nature* 411(6839):789-792.
19. Sala A, Piper F, & Hoch G (2010) Physiological mechanisms of drought-induced tree mortality are far from being resolved. *New Phytologist* 186(2):274-281.
20. Gavito ME, Jakobsen I, Mikkelsen TN, & Mora F (2019) Direct evidence for modulation of photosynthesis by an arbuscular mycorrhiza-induced carbon sink strength. *New Phytologist* 223(2):896-907.
21. Hommel R*, et al.* (2016) Impact of interspecific competition and drought on the allocation of new assimilates in trees. *Plant Biology* 18(5):785-796.
22. Körner C (2015) Paradigm shift in plant growth control. *Current Opinion in Plant Biology* 25:107-114.
23. Fabre D*, et al.* (2019) Is triose phosphate utilization involved in the feedback inhibition of photosynthesis in rice under conditions of sink limitation? *Journal of Experimental Botany* 70(20):5773-5785.
24. Bardgett RD, Bowman WD, Kaufmann R, & Schmidt SK (2005) A temporal approach to linking aboveground and belowground ecology. *Trends in Ecology & Evolution* 20(11):634-641.
25. Schönbeck L*, et al.* (2018) Homeostatic levels of nonstructural carbohydrates after 13 yr of drought and irrigation in Pinus sylvestris. *New Phytologist* 219(4):1314-1324.
26. George E & Marschner H (1996) Nutrient and water uptake by roots of forest trees. *Zeitschrift für Pflanzenernährung und Bodenkunde* 159(1):11-21.
27. Epron D*, et al.* (2012) Pulse-labelling trees to study carbon allocation dynamics: a review of methods, current knowledge and future prospects. *Tree Physiology* 32:776-798.
28. Desalme D*, et al.* (2017) Seasonal variations drive short-term dynamics and partitioning of recently assimilated carbon in the foliage of adult beech and pine. *New Phytologist* 213(1):140-153.
29. Sevanto S (2014) Phloem transport and drought. *Journal Of Experimental Botany* 65(7):ert467-1759.
30. Manzoni S, Schimel JP, & Porporato A (2012) Responses of soil microbial communities to water stress: results from a meta-analysis. *Ecology* 93(4):930-938.
31. Brunner I, Herzog C, Galiano L, & Gessler A (2019) Plasticity of Fine-Root Traits Under Long-Term Irrigation of a Water-Limited Scots Pine Forest. *Frontiers in plant science* 10:701-701.
32. Finér L, Ohashi M, Noguchi K, & Hirano Y (2011) Factors causing variation in fine root biomass in forest ecosystems. *Forest Ecology and Management* 261(2):265-277.
33. Brunner I, Herzog C, Dawes MA, Arend M, & Sperisen C (2015) How tree roots respond to drought. *Frontiers in Plant Science* 6:547.

34. Carteron A, Beigas M, Joly S, Turner BL, & Laliberté E (2020) Temperate Forests Dominated by Arbuscular or Ectomycorrhizal Fungi Are Characterized by Strong Shifts from Saprotrophic to Mycorrhizal Fungi with Increasing Soil Depth. *Microbial Ecology*.
35. Germon A, Laclau J-P, Robin A, & Jourdan C (2020) Tamm Review: Deep fine roots in forest ecosystems: Why dig deeper? *Forest Ecology and Management* 466:118135.
36. López B, Sabaté S, & Gracia CA (2001) Vertical distribution of fine root density, length density, area index and mean diameter in a Quercus ilex forest. *Tree Physiology* 21(8):555-560.
37. Brunner I*, et al.* (2009) Morphological and physiological responses of Scots pine fine roots to water supply in a dry climatic region in Switzerland. *Tree Physiology* 29(4):541-550.
38. Rigling A*, et al.* (2013) Driving factors of a vegetation shift from Scots pine to pubescent oak in dry Alpine forests. *Global Change Biology* 19(1):229-240.
39. Scholander PF, Bradstreet ED, Hemmingsen EA, & Hammel HT (1965) Sap Pressure in Vascular Plants. *Science* 148:339-346.
40. Bamberger I*, et al.* (2017) Isoprene emission and photosynthesis during heatwaves and drought in black locust. *Biogeosciences* 14(15):3649-3667.
41. Brandes E*, et al.* (2006) Short-term variation in the isotopic composition of organic matter allocated from the leaves to the stem of *Pinus sylvestris*: effects of photosynthetic and postphotosynthetic carbon isotope fractionation. *Global Change Biology* 12(10):1922-1939.
42. Subke JA*, et al.* (2004) Feedback interactions between needle litter decomposition and rhizosphere activity. *Oecologia* 139(4):551-559.
43. Zeeman MJ*, et al.* (2008) Optimization of automated gas sample collection and isotope ratio mass spectrometric analysis of δ13C of CO2 in air. *Rapid Communications in Mass Spectrometry* 22(23):3883-3892.
44. Lang SQ, Bernasconi SM, & Früh-Green GL (2012) Stable isotope analysis of organic carbon in small (µg C) samples and dissolved organic matter using a GasBench preparation device. *Rapid Communications in Mass Spectrometry* 26(1):9-16.
45. Högberg P*, et al.* (2008) High temporal resolution tracing of photosynthate carbon from the tree canopy to forest soil microorganisms. *New Phytologist* 177(1):220-228.
46. Hoch G, Richter A, & Körner C (2003) Non-structural carbon compounds in temperate forest trees. *Plant, Cell and Environment* 26(7):1067-1081.
47. Forrester DI*, et al.* (2017) Generalized biomass and leaf area allometric equations for European tree species incorporating stand structure, tree age and climate. *Forest Ecology and Management* 396:160-175.

Tables

Table 1: Results of the linear mixed effects models testing the effects of precipitation, irrigation and their interaction on soil water content, predawn leaf water potential, gas exchange parameters, total $^{13}CO_2$ taken up and the relative allocation of ^{13}C to belowground pools and soil respiration. DF= Degrees of freedom (num DF, denom DF); ** = $P < 0.01$, * = $P < 0.05$. Leaf water potential was measured only before the rainfall event (see **SI Appendix, Fig. S4**)

Parameters	Fixed effects	DF	*F*-value	*P*-value
Soil water content (0-5 cm) *(g H_2O g^{-1} soil)*	Precipitation	1,3	11.9	0.040*
	Irrigation	1,3	57.3	0.004***
	Precipitation x Irrigation	1,3	2.9	0.18
Leaf water potential *(MPa)*	Irrigation	1,3	25.2	0.007**
Photosynthesis *(µmol m^{-2} s^{-1})*	Precipitation	1,3	0.05	0.84
	Irrigation	1,3	1.9	0.30
	Precipitation x Irrigation	1,3	14.4	0.06
Stomatal conductance *(mmol m^{-2} s^{-1})*	Precipitation	1,3	0.13	0.75
	Irrigation	1,3	1.94	0.300
	Precipitation x Irrigation	1,3	0.86	0.45
Transpiration *(mmol m^{-2} s^{-1})*	Precipitation	1,3	0.18	0.70
	Irrigation	1,3	4.14	0.17
	Precipitation x Irrigation	1,3	0.68	0.49
Total ^{13}C-CO_2 assimilated *(g)*	Precipitation	1,3	11.4	0.042*
	Irrigation	1,3	2.9	0.19
	Precipitation x Irrigation	1,3	0.1	0.76
^{13}C allocation to belowground pools *(%)*	Precipitation	1,3	3.0	0.17
	Irrigation	1,3	13.1	0.01*
	Precipitation x Irrigation	1,3	69.2	0.006**
^{13}C allocation to soil respiration *(%)*	Precipitation	1,3	0.13	0.73
	Irrigation	1,3	34.3	0.009**
	Precipitation x Irrigation	1,3	11.4	0.04*

Figure legends

Figure 1: Setup of the ^{13}C pulse labelling (left side) and the tracing of the fate of ^{13}C in respiratory fluxes and plant and soil microbial pools (right side). A transparent plastic sheet was erected from scaffolds, enclosing the whole tree crown to form a labelling chamber. $^{13}CO_2$ was added to the chamber from gas bottles via a mass flow controller. The $^{13}CO_2$ concentration was monitored with LGR CCIA 46d isotope laser spectrometers. The air temperature was adjusted to maintain ambient temperature with an air conditioning system involving a closed coolant system so that no air exchange between inside and outside the chamber occurred. One branch, stem and soil chamber per tree were connected via a manifold with automatically controlled solenoid valves to the isotope laser spectrometer. Within a radius of 8 m (along three transects per tree), soil collars were installed to determine the spatio-temporal pattern of soil-respired $^{13}CO_2$ that was measured in gas samples. Samples of different plant organs and the soil microbial biomass were taken to determine the ^{13}C enrichment at different time points after labelling.

Figure 2: Dynamics of water-soluble carbohydrates in root tissues and of ^{13}C in soil-respired CO_2 and microbial biomass before and after the rainfall event. (a) shows the ratio of root soluble sugars between trees from naturally dry non-irrigated and irrigated plots before as well as 3 days and 2 weeks after the rainfall event. The data for the time before the rainfall event were taken from[18] where root samples were collected during a dry period in summer. (b) and (c) show the temporal course of ^{13}C in the soil CO_2 flux in the non-irrigated, and the irrigated plots after pulse labelling (at t = 0 days) before and after the rainfall event. Similarly, (d), and (e) show the ^{13}C-incorporation into soil microbial biomass (on a m^2 soil surface basis) in the non-irrigated, and irrigated plots labelled before or after the rainfall event. Error bars indicate SD in (a) and SE in (b)-(e). * in (a) indicates significant differences at $p < 0.05$ according to student's *t*-test (n = 3).

Figure 3. Relative distribution of the recently assimilated ^{13}C from pulse labelling applied before and after the rainfall event. The percentage of total assimilated ^{13}C recovered in different pools and fluxes, as well as the overall above- and belowground distribution are shown in irrigated and non-irrigated plots. Aboveground fluxes comprise canopy plus stem respiration, while aboveground biomass pools include structural and non-structural C from needles, branches and the stem (for individual values see **SI Appendix, Tab. S2**). Belowground pools comprise structural and non-structural C from roots plus the soil microbial biomass (for individual values see **SI Appendix, Tab. S2**). Data shown are integrated fluxes until day 30 after the application of the pulse labelling and the recovery in the pools harvested at day 30. Arrow widths (indicating fluxes) and bars (indicating the overall below- and aboveground distribution) scale proportionally. Aboveground flux data after the rainfall event were not directly measured but calculated as described in the Supplementary Methods section. Both, the relative allocation of new assimilates to total belowground pools and fluxes and to belowground respiration in particular were significantly affected by the irrigation treatment (belowground pool $p = 0.01$; soil respiration $p = 0.009$) but also by the interaction between irrigation treatment and the rainfall event (belowground pool $p = 0.006$; soil respiration $p = 0.04$; for detailed statistical information see **Tab. 1** and **SI Appendix, Tab. S2**).

Figure 4: Effect of soil moisture availability on microbial C mineralization (=heterotrophic respiration) rate (a), and on cumulative belowground respiration of recent assimilates (b). In (a) soil microbial respiration was determined in soil samples (excluding roots) from three different depths (0-2, 2-5 and 5-10 cm) at different soil moisture levels adjusted under controlled conditions. In (b) soil ^{13}C-CO_2 flux cumulated over the 30 days after the pulse labelling is depicted against the soil water content at 2-10 cm depth shortly after labelling. Here the variation of the soil moisture is affected by treatment (irrigation vs. non irrigation), the precipitation event and the spatial variability. The dashed line in (a) represents the fit of microbial respiration from root-free soil (normalized to maximal rates) to a Boltzmann equation that was then scaled in (b) to rhizosphere respiration without changing moisture dependencies. r^2 is the coefficient of determination and ** depicts $p < 0.01$ and *** $p < 0.001$.

ORCID:

Jobin Joseph: https://orcid.org/0000-0002-6342-2505
Ivano Brunner: https://orcid.org/0000-0003-3436-995X
Gerd Gleixner: https://orcid.org/0000-0002-4616-0953
Henrik Hartmann: https://orcid.org/0000-0002-9926-5484
Ansgar Kahmen: https://orcid.org/0000-0002-7823-5163
Mai-He Li: https://orcid.org/0000-0002-7029-2841
Martina Peter: https://orcid.org/0000-0002-6365-6889
Christian Poll: https://orcid.org/0000-0002-9674-4447
Andreas Rigling: https://orcid.org/0000-0003-1944-4042
Kaisa A Rissanen: https://orcid.org/0000-0002-8615-4195
Nadine Ruehr: https://orcid.org/0000-0001-5989-7463
Matthias Saurer: https://orcid.org/0000-0002-3954-3534
Marcus Schaub: https://orcid.org/0000-0002-0158-8892
Leonie Schönbeck: https://orcid.org/0000-0001-9576-254X
Frank M Thomas: https://orcid.org/0000-0003-3697-714X
Thomas Wohlgemuth: https://orcid.org/0000-0002-4623-0894
Frank Hagedorn: https://orcid.org/0000-0001-5218-7776
Arthur Gessler: https://orcid.org/0000-0002-1910-9589

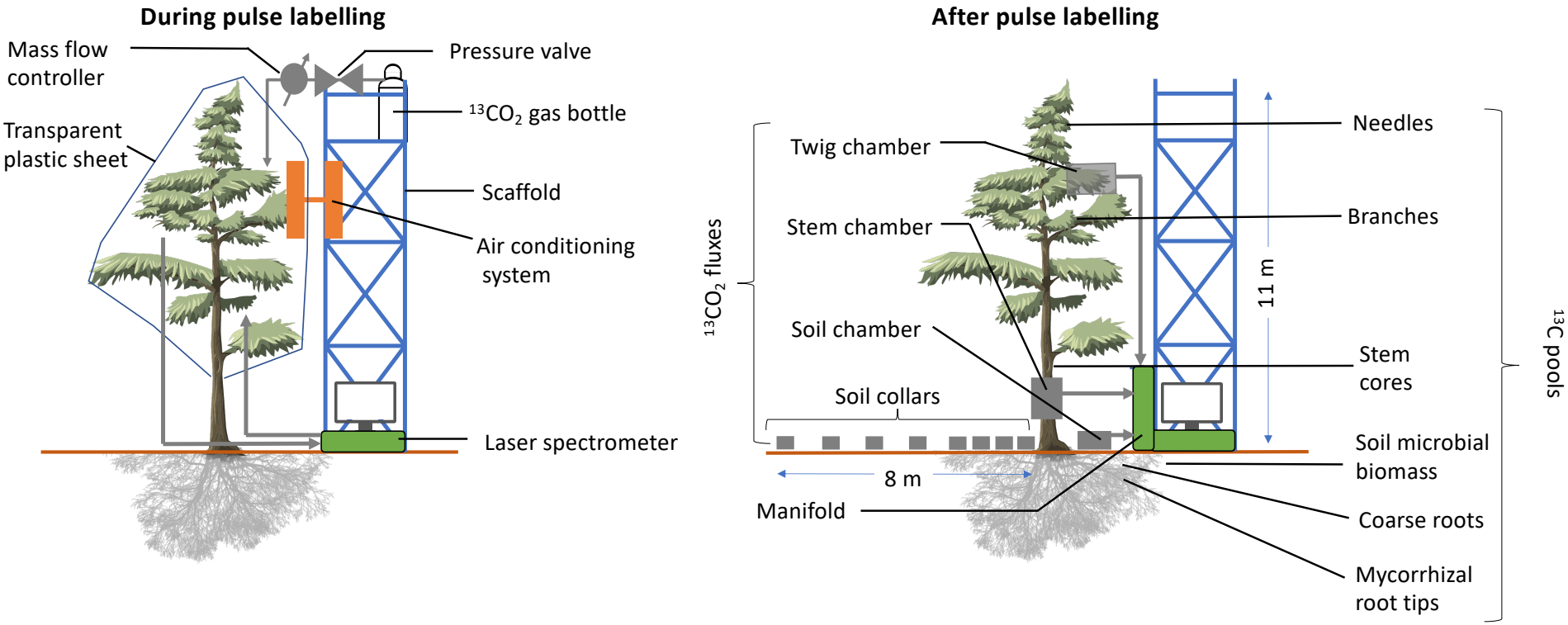
During pulse labelling
Mass flow controller
Pressure valve
$^{13}CO_2$ gas bottle
Transparent plastic sheet
Scaffold
Air conditioning system
Laser spectrometer
After pulse labelling
$^{13}CO_2$ fluxes
Twig chamber
Stem chamber
Soil chamber
Soil collars
8 m
Manifold
11 m
Needles
Branches
Stem cores
Soil microbial biomass
Coarse roots
Mycorrhizal root tips
^{13}C pools

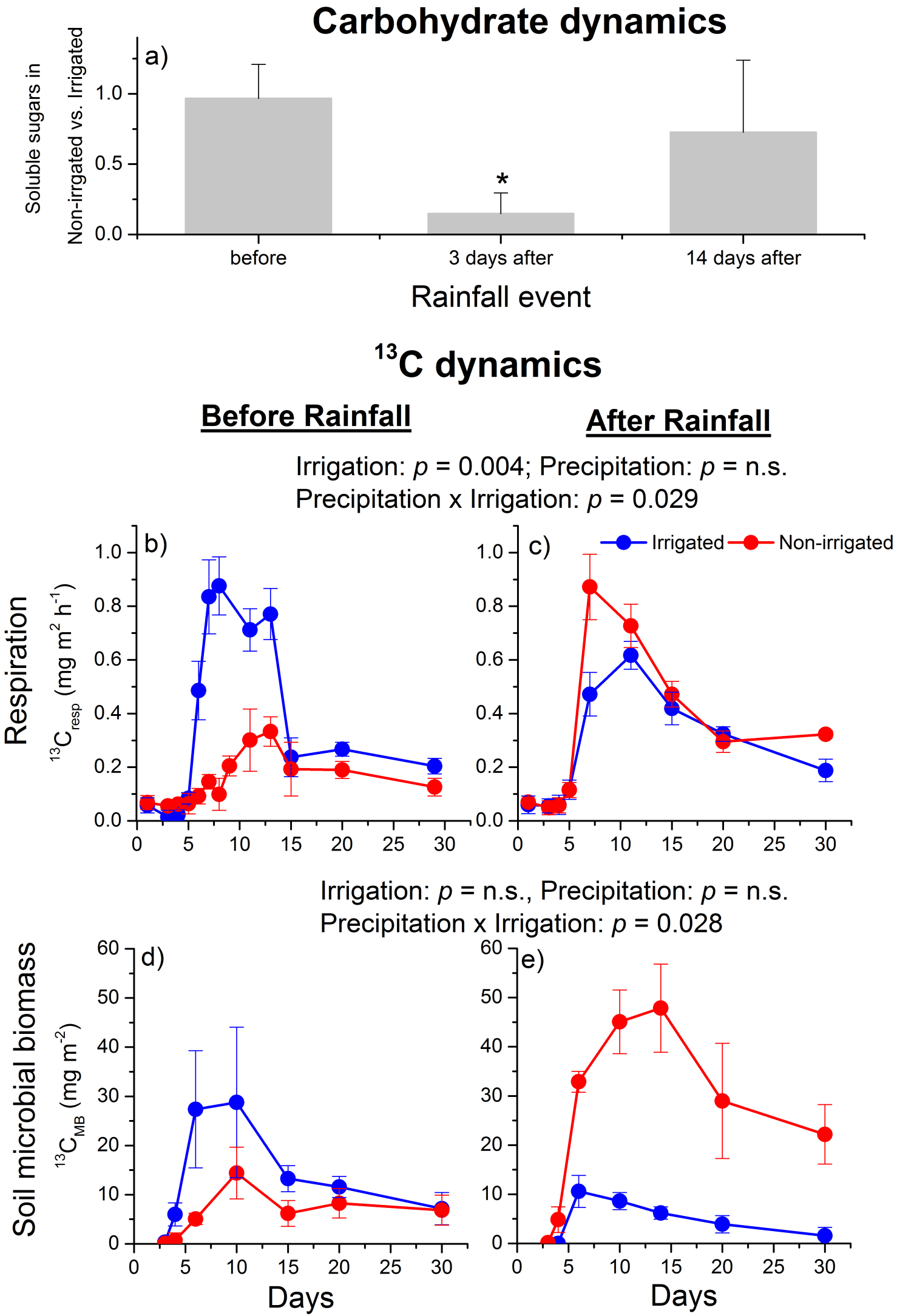
Carbohydrate dynamics
a)
Soluble sugars in Non-irrgated vs. Irrigated
1.0
0.5
0.0
*
before
3 days after
14 days after
Rainfall event
13C dynamics
Before Rainfall
After Rainfall
Irrigation: p = 0.004; Precipitation: p = n.s.
Precipitation x Irrigation: p = 0.029
Respiration
b)
c)
Irrigated
Non-irrigated
13Cresp (mg m2 h-1)
1.0
0.8
0.6
0.4
0.2
0.0
0
5
10
15
20
25
30
Irrigation: p = n.s., Precipitation: p = n.s.
Precipitation x Irrigation: p = 0.028
Soil microbial biomass
d)
e)
13CMB (mg m-2)
60
50
40
30
20
10
0
Days

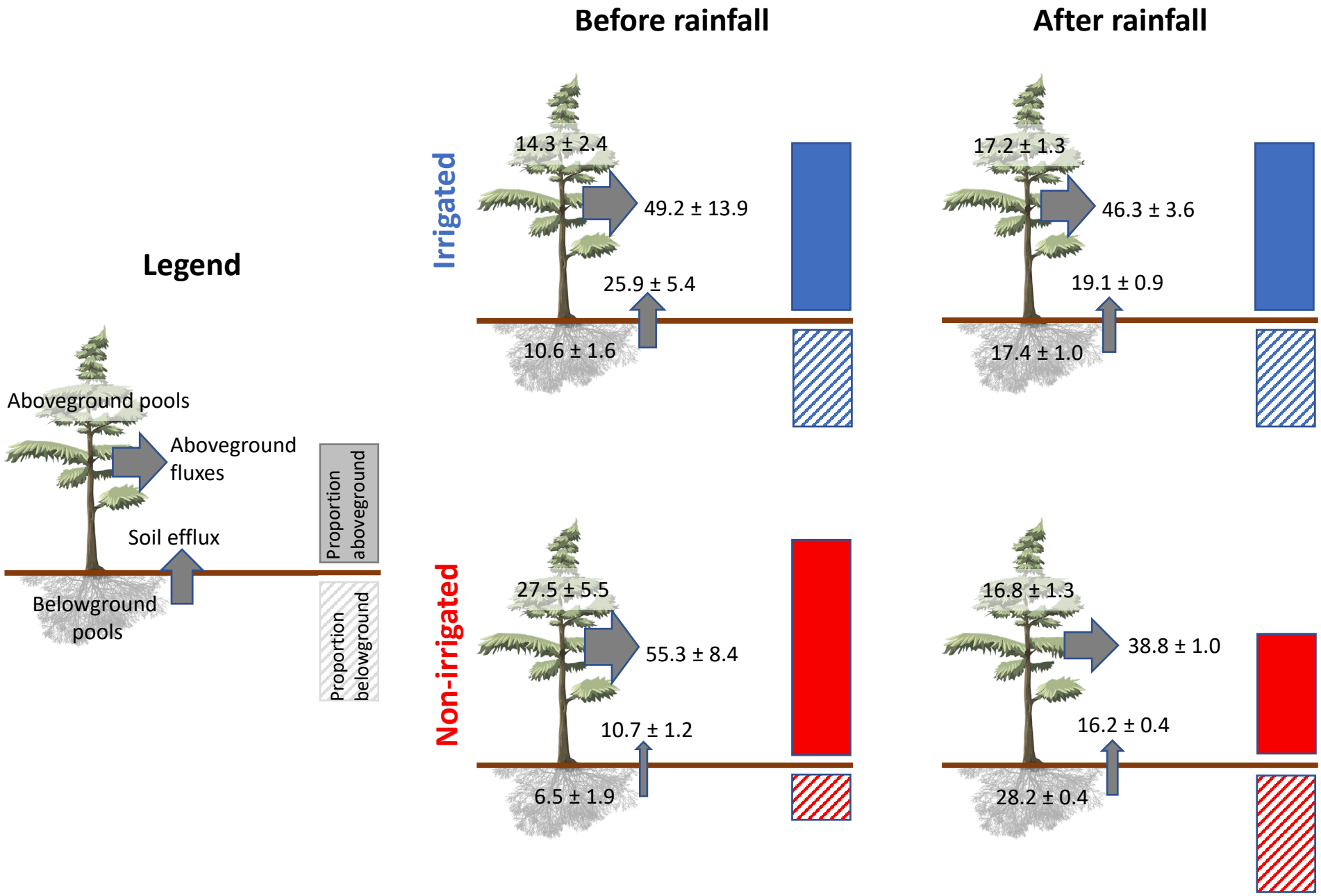
Before rainfall
After rainfall
Legend
Aboveground pools
Aboveground fluxes
Soil efflux
Belowground pools
Proportion aboveground
Proportion belowground
Irrigated
14.3 ± 2.4
49.2 ± 13.9
25.9 ± 5.4
10.6 ± 1.6
17.2 ± 1.3
46.3 ± 3.6
19.1 ± 0.9
17.4 ± 1.0
Non-irrigated
27.5 ± 5.5
55.3 ± 8.4
10.7 ± 1.2
6.5 ± 1.9
16.8 ± 1.3
38.8 ± 1.0
16.2 ± 0.4
28.2 ± 0.4

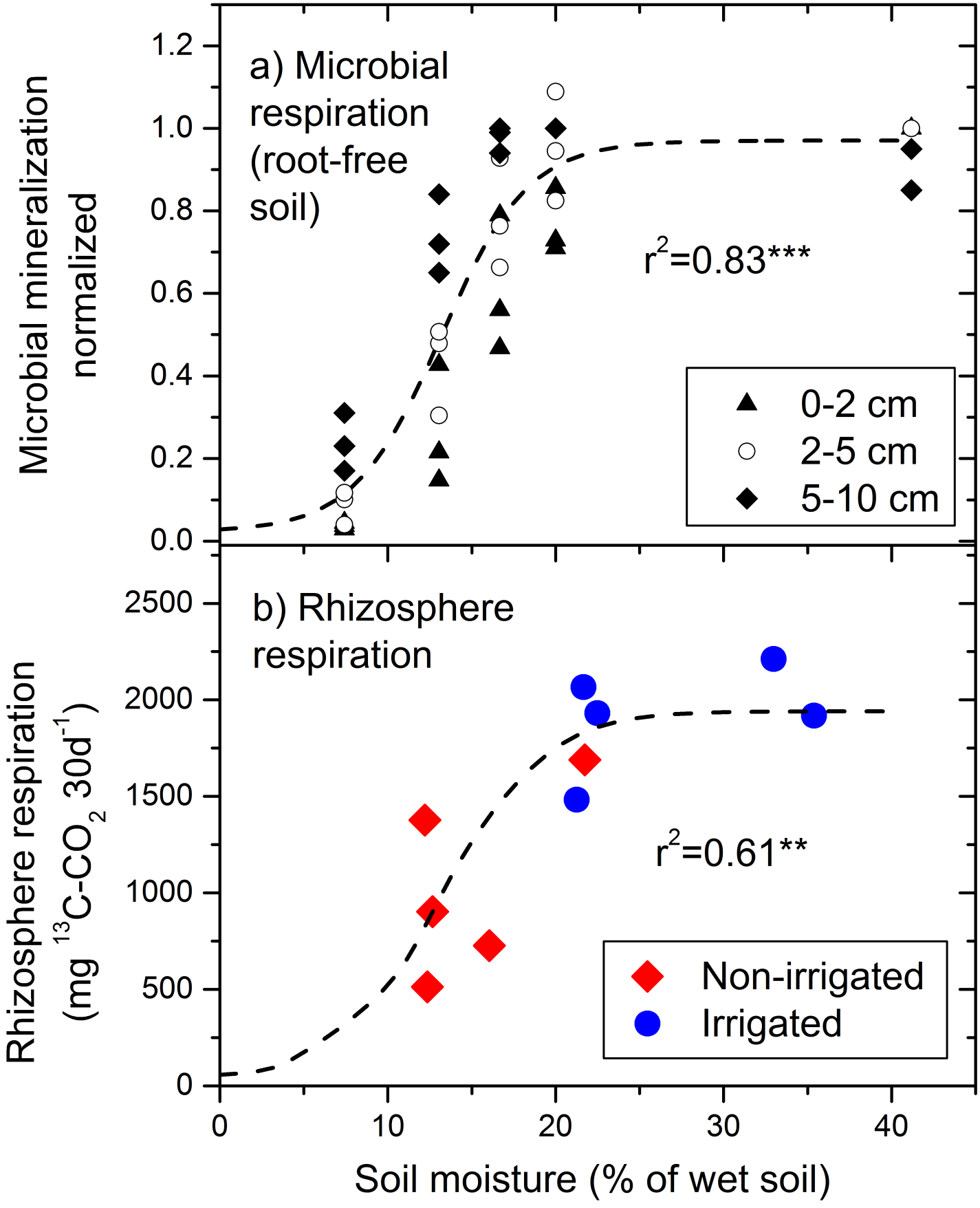
a) Microbial respiration (root-free soil)
r²=0.83***
0-2 cm
2-5 cm
5-10 cm
Microbial mineralization normalized
1.2
1.0
0.8
0.6
0.4
0.2
0.0
b) Rhizosphere respiration
r²=0.61**
Non-irrigated
Irrigated
Rhizosphere respiration (mg ¹³C-CO₂ 30d⁻¹)
2500
2000
1500
1000
500
0
0
10
20
30
40
Soil moisture (% of wet soil)